Mon. Not. R. Astron. Soc. **270,** 121–130 (1994)

A possible criterion for envelope ejection in asymptotic giant branch or first giant branch stars

Zhanwen Han, Philipp Podsiadlowski and Peter P. Eggleton
Institute of Astronomy, Madingley Road, Cambridge CB3 0HA

Accepted 1994 April 15. Received 1994 April 13; in original form 1993 December 20

ABSTRACT

Following Paczyński & Ziółkowski, we investigate the relationship between the zero-age mass of a star and the mass of its degenerate core at that point in the star's evolution when the binding energy of its envelope changes from negative to positive. This relationship is fairly consistent, to within observational error, with the relationship by Weidemann & Koester between the initial mass and the mass of the white dwarf (WD) remnant, and with the observed distribution of masses of planetary nebula nuclei. We derive the equivalent relation for Population II (Pop II) stars ($Z = 0.001$), finding white dwarf masses ~10–20 per cent greater for the same initial masses. For both Population I (Pop I) and Pop II, however, we do not obtain C/O WD masses above $\sim 1.1\,M_\odot$ – the putative massive progenitors ($\gtrsim 8$ and $6\,M_\odot$ respectively) have negative envelope binding energies even at fairly extreme red supergiant radii. For low-mass Pop I stars ($\lesssim 1\,M_\odot$), we obtain He WD remnants by the same process on the first giant branch. We discuss the implications of our calculations for C/O WD masses, thermonuclear Type II supernovae, and the use of planetary nebulae as distance candles.

Key words: stars: AGB and post-AGB – stars: evolution – stars: mass-loss – white dwarfs – planetary nebulae: general.

1 INTRODUCTION

Paczyński & Ziółkowski (1968, hereinafter PZ) suggested that the envelope of a star on the asymptotic giant branch (AGB) may be blown off at that stage in the star's evolution when the binding energy of the envelope changes from negative to positive – see also Biermann (1938), Biermann & Cowling (1939), Shklovskiĭ (1956), Lucy (1967) and Roxburgh (1967). The present authors, as part of a study of the possible common-envelope evolution (Paczyński 1976) of moderately wide binary stars, have computed the evolution of a number of stars from the zero-age main sequence (ZAMS) to the top of the AGB, determining among other things the binding energy of the envelope as it evolves. We therefore obtain a relation between M_i, the initial mass of a star, and the value M_f of the core mass M_c at that point on the AGB where the binding energy passes through zero. The result appears to us to be quite close to the observationally based relation by Weidemann & Koester (1983, hereinafter WK) between M_i and M_f, the latter in their context being the mass of the white dwarf (WD) remnant associated with a star of initial mass M_i. It also predicts a distribution of masses of planetary nebula nuclei which is in good agreement with the observed one (see Section 3). Thus we believe that we may have confirmed the rather natural hypothesis of PZ. Recently, Wagenhuber & Weiss (1993) have independently reinvestigated the hypothesis of PZ and arrived at a similar conclusion.

The connection between binding energy (BE) and envelope ejection is not, however, especially direct. There appear to be four major areas of uncertainty.

(i) The BE of an entire star is well known to be

$$W = \int_0^{M_s} \left(-\frac{Gm}{r} + U \right) \mathrm{d}m, \qquad (1)$$

where U is the internal energy of thermodynamics (involving terms due to ionization of H and dissociation of H_2, as well as the basic $\frac{3}{2}\Re T/\mu$ for a simple perfect gas, and the Fermi energy of a degenerate electron gas), and M_s is the surface value of the mass coordinate m. It is not, however, axiomatically true that the BE of the envelope outside some core of mass M_c is the corresponding integral from M_c to M_s, since during the supposed loss of the envelope the structure of the core may change, and thus absorb or release energy. However, if the core closely resembles a white dwarf structure, whose distributions of density, pressure and internal energy

depend very little on temperature, then we think it is reasonable to suppose that its energy will not change during the loss of the envelope, and so we take the BE of the envelope to be

$$\Delta W = \int_{M_c}^{M_s} \left(-\frac{Gm}{r} + U \right) \mathrm{d}m. \qquad (2)$$

In Section 2 we discuss the procedure that we use for defining M_c. Subsequently, we use M_f to mean the value of this M_c when $\Delta W = 0$, begging the question whether this is the same M_f as the empirical final masses of WK.

(ii) Modelling of the AGB envelope is necessarily somewhat crude. We use the mixing-length theory of convection (with $\alpha = 2$, see below), and a surface boundary condition which assumes plane-parallel temperature stratification, negligible mass above the photosphere, and constant opacity there. These assumptions are generally quite good for dwarfs, but are known to be much weaker for the distended envelopes of AGB stars.

(iii) Most stellar evolutionary codes require short time-steps during AGB evolution, and then show the well-known relaxation cycles of 'thermal shell flashes' (Schwarzschild & Härm 1965). Our code, based on Eggleton (1971, 1972, 1973) although much modified over the course of 20 years, can take long time-steps, say 1 per cent of the nuclear time-scale of the star, and thus does not develop shell flashes (unless we reduce the time-step by a factor of ~50: R. C. Cannon, private communication). It is not clear that our AGB models, in which both of the nuclear-burning shells march steadily outwards very close together when the He shell has caught up with the H shell, represent the best 'average' of the actual cyclic behaviour. It is certainly not clear, however, that there is any more plausible 'average' to be obtained.

(iv) Although in principle when $\Delta W > 0$ the envelope has sufficient energy to disappear to infinity, it is not clear that this loss of envelope will actually take place. Some of the energy that would be required to go into outward motion in order to achieve this might actually be radiated away, before the envelope has expanded much. We might, rather, expect a series of oscillations on a dynamical time-scale (presumably Mira pulsations), with amplitude growing on a nuclear time-scale until ΔW is large enough to energize envelope ejection despite radiative losses.

Notwithstanding these uncertainties, we press on with the simple question: what is the relation between M_i and the M_c at which $\Delta W = 0$? The answer to this question seems to us to be sufficiently close to the observationally based WK relation that we feel that the uncertainties may not in fact be overwhelming.

2 METHOD

The evolutionary code of Eggleton (1971, 1972, 1973) has undergone several modifications over the course of 20 years, and so we take this opportunity to describe briefly the present version. What is unchanged is the basic philosophy, that we solve for all of (i) the composition, (ii) the mesh-point distribution, and (iii) the structure, in a single implicit Newton–Raphson iterative step. However, we now follow four main nuclear species rather than just one, while economizing on equations and hence cpu time by using a second-order difference equation for each species instead of two first-order equations. The nuclear species that we follow are ^{1}H, ^{4}He, ^{12}C and ^{16}O. Transient equilibrium is assumed for several other species, e.g. ^{2}H, ^{3}He, ^{13}C; other species are ignored. Rates for the 10 nuclear reactions involved are taken from Fowler, Caughlan & Zimmerman (1976). Each of the four main species is distributed in the star according to a diffusion-like approximation for convective (including semi-convective) mixing (Eggleton 1971, 1983). The diffusion coefficient used to model convective mixing is considerably weaker than the mixing-length convection theory would imply. This is simply for numerical convenience. The mixing is still rapid enough to make the composition uniform to about 1 part in 10^3 in convective regions, as against perhaps 1 part in 10^{10} which might be expected more realistically. We do not believe that the difference between 10^{-3} and 10^{-10} is significant. Semiconvection is included automatically in the same diffusive approximation, since we solve for the structure and the composition simultaneously and implicitly.

It is sometimes supposed that such a code, involving the simultaneous solution of nine implicit difference equations, some first-order and some second-order, must be more complex than more usual codes which solve only four implicit first-order equations for the structure alone. In fact, this is the opposite of the truth: by solving for the structure, composition and mesh-point distribution simultaneously, so many problems go away that one is left with a very simple code. There is no need for ad hoc procedures for shifting thin burning shells, adding or subtracting mesh-points, locating the boundaries between convective, semiconvective and radiative zones, or separating the envelope structure from the interior, for example. Thus the code needs only ~1500 lines of FORTRAN, perhaps an order of magnitude less than some codes of a more traditional variety. This has the further advantage of making the code much easier to modify for special purposes.

The implicitly computed distribution of mesh-points gives a mesh which is sometimes called 'adaptive'. The points are located at equal intervals of a function of p, T and m which has been determined by experience to give an adequate dissection for a star of any mass, and at any evolutionary stage between the ZAMS (or earlier) and the tip of the AGB, where the core mass approaches the Chandrasekhar limit; or, in massive stars, from the ZAMS to the end of carbon burning. Only 200 mesh-points appear to be necessary, distributed between the centre and the photosphere (defined as the point where optical depth is 2/3). About 3000 to 5000 time-steps are necessary for a complete evolutionary run, or substantially less if one is prepared to intervene manually once or twice.

The code is very stable numerically, provided that the star is not varying on a time-scale several times shorter than the usual thermal time-scale. The time-steps are generally dictated by the overall *nuclear* time-scale, except in phases such as the first crossing of the Hertzsprung gap which are inherently on a thermal time-scale. Partly because of the stability, and partly because hydrostatic equilibrium is assumed, the code does not pick up short-time-scale behaviour such as Cepheid or Mira pulsations, or shell flashes. This may not

always be an advantage, but it does allow us to compute rapidly an approximation to the AGB phase, where most other codes are slowed down very considerably by having to follow the shell flashes in detail.

The implicit difference scheme is centrally differenced, except to the extent that advection terms are approximated by 'upstream' differencing, which is vital for shell-burning phases (single or double). The central difference character is probably responsible for breakdown during degenerate core ignition, whether He or C. Degenerate He ignition happens below $\sim 2.3\,M_\odot$ (Pop I; $X=0.7$, $Z=0.02$) or $\sim 1.9\,M_\odot$ (Pop II; $X=0.75$, $Z=0.001$), and degenerate C ignition below $\sim 8\,M_\odot$ (Pop I) or $\sim 6\,M_\odot$ (Pop II). For our 'zero-age horizontal branch' models, i.e. post-He-flash stars of $\lesssim 2.3\,M_\odot$, we used models obtained by (i) first evolving a star of $3\,M_\odot$ to (non-degenerate) He ignition, (ii) causing it to lose mass artificially until its total mass was what was required, and (iii) allowing the H shell to burn outwards until the He core had the mass that had been reached at the He core flash. During these three steps the nuclear energy released by He burning was included, but not the effect on the composition, so that the star restarted its evolution with a core of uniform composition.

We used the opacities by Rogers & Iglesias (1992, hereinafter OPAL) for $Z=0.02$ (Pop I) and $Z=0.001$ (Pop II), except that we replaced them at low temperatures by molecular opacities taken from Weiss, Keady & Magee (1990, hereinafter WKM). The latter tables are not especially comprehensive, however, except for the two metallicities that we adopted. Dr A. Weiss kindly provided a version interpolated to the temperature–density grid that we used. Degenerate electron conduction was taken from Hubbard & Lampe (1969).

Molecular opacities are of course very important in the structure of cool stars, such as AGB stars. Our AGB differs in shape and location quite substantially from those of models using the same code but earlier opacity tables without molecules. Generally, our AGB tracks curve more strongly to progressively lower temperature at a given luminosity than do earlier tracks, which were generally fairly straight when plotted in a theoretical Hertzsprung–Russell diagram (HRD). We needed a mixing-length ratio α of 2 to get a roughly correct lower main sequence (MS), as determined observationally by Andersen (1991), although even with this value (large by the standards of the 1960s to 1980s, but not any more unlikely a priori) we still get a model at $1\,M_\odot$ which is a little cooler and less luminous than the Sun. We have not attempted a more definitive calibration. However, our models well reproduce the location of the red giant branch in the HRD for stars in the Hyades supercluster (Eggen 1985), as determined by Bessell et al. (1989).

Because our models are of too low a zero-age luminosity at $\sim 1\,M_\odot$, our nuclear lifetimes for stars near this mass are uncomfortably long, more like 15 than 10 Gyr. We would like to be able to fine-tune X, Z and α so as to get the Sun right, but our opacity table does not give us the freedom to vary Z. Dr C. A. Tout (private communication) tells us that for $Z=0.02$ our opacity table requires us to take $\alpha=2.5$ and $X=0.67$ in order to get a good solar model at age 4.65 Gyr; this model then has a convective envelope depth of $0.29\,R_\odot$, which is in good agreement with solar oscillation data (Christensen-Dalsgaard, Gough & Thompson 1991). We are not aware of any other modelling of the Sun that takes account of molecular opacities at lower temperatures as well as OPAL opacities at higher temperatures.

The equation of state is largely that described by Eggleton, Faulkner & Flannery (1973), but with the inclusion of molecular hydrogen, and some improvement in the treatment of pressure dissociation (which nevertheless remains rather crude and simple). It does not include the ionization of species other than H or He, nor dissociation of molecules other than H_2; all atomic species other than H and He are assumed to be fully ionized. Coulomb lattice effects in the degenerate core are not included, nor are the following processes at very high temperature and/or density: inverse β-decay, pair production, and photodissociation of nuclei.

In Section 1 we alluded to the fact that it is not entirely obvious how we should determine M_c, the lower limit of the integral in equation (2) which determines the binding energy. The process we use is illustrated in Fig. 1, which shows ΔW as a function of M_c, at two stages of evolution of an AGB star of $2\,M_\odot$. It can be seen that there are three portions of each curve: (i) an inner region where ΔW increases slowly; (ii) a zone (which includes the H-burning shell) where ΔW increases sharply; and then (iii) an outer portion where ΔW varies fairly slowly again with M_c. We feel that the best choice of M_c is a value near but outside the transition between (ii) and (iii). With this choice we ensure that ΔW is not very sensitive to M_c, and varies in a systematic manner both with evolutionary stage for a given total mass and with total mass at a given evolutionary stage.

3 RESULTS

In Fig. 2(a) we show the relation we obtain between M_i and M_f, for Pops I and II. For the two lowest values of M_i, in Pop I only, we obtain two points each, because the star just reached $\Delta W=0$ on the first giant branch (FGB) as well as on the AGB. Our M_i–M_f relation is reasonably approximated by three straight-line segments, thus:

$$M_f = \max[0.54+0.042M_i, \min(0.36+0.104M_i, 0.58+0.061M_i)], \qquad 0.8 \lesssim M_i \lesssim 7.5\,M_\odot \quad (3)$$

for Pop I, and

$$M_f = \max[0.54+0.073M_i, \min(0.29+0.178M_i, 0.65+0.062M_i)], \qquad 0.8 \lesssim M_i \lesssim 6.3\,M_\odot \quad (4)$$

for Pop II; except that for Pop I, with $0.8 \lesssim M_i \lesssim 1\,M_\odot$, there is a lower alternative value of $\sim 0.46\,M_\odot$, if the envelope is indeed lost on the FGB. Figs 2(b) and (c) show final radius and final luminosity, also as functions of M_i, and Fig. 2(d) shows the termination points of our tracks on the theoretical HRD.

WK's observational M_i–M_f relation was based on 13 WDs, all but one in Galactic clusters: the nearby WD 40 Eri B, five in the Hyades, two in NGC 2287, one in the Pleiades, one in NGC 2422 and three in NGC 2516. The individual points in WK's fig. 1 (several of which are different and somewhat discordant measures of the same WD) show a very considerable scatter, but all lie roughly between the two dashed lines in our Fig. 2(a). Probably the observed WD masses are uncertain by ~ 20 per cent, and the inferred initial masses must be considerably more uncertain. Note

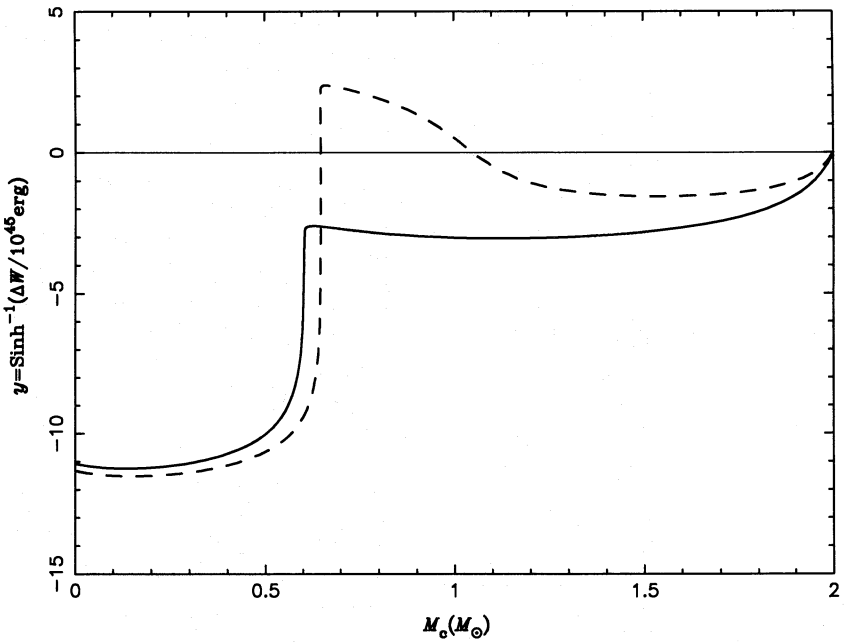

Figure 1. The envelope binding energy ΔW (equation 2), as a function of M_c at two stages of evolution of an AGB star of 2 $M_\odot$. The dependent variable, $y = \sinh^{-1}(\Delta W/10^{45}$ erg), keeps the sign of $\Delta W/10^{45}$ erg and is a logarithmic function of $\Delta W/10^{45}$ erg when its absolute value is large, or a linear function when its absolute value is small.

that even the 'observed' initial masses require a substantial amount of theoretical input. For the most part they are obtained by consideration of the age (from stellar modelling) of the cluster to which the WD belongs. The cooling time, also from stellar modelling (Koester 1972), for the WD to reach its present luminosity is subtracted from the cluster age, thus giving the lifetime of the progenitor star, and hence (again from stellar modelling) the progenitor's mass. This mass will therefore depend on what models were used. Our own models, using the OPAL+WKM opacities, differ appreciably from earlier models, and in particular seem to give a broader MS at moderate masses. This should reduce, and perhaps even eliminate, the necessity for convective overshooting, which was incorporated in the models of Maeder & Mermilliod (1981), on which much of WK's analysis was based. However, the effect on estimates of M_i should not be large: since lifetime depends strongly on initial mass and only moderately on opacity etc., it follows that initial masses are fairly tightly constrained by lifetime estimates.

Given the uncertainties, therefore, we feel that the agreement between our relation for Pop I and WK's relation is quite reasonable. We have, however, also attempted to incorporate the effect on our models of a steady stellar wind, based on the observational relation given by Judge & Stencel (1991, hereinafter JS). These authors presented several least-squares fits of observed mass-loss rates in red giants to various formulae involving L, R and m. Their preferred estimate (which of course also shows considerable scatter) is

$$-\dot{m} \sim 10^{-13.6}\left(\frac{r^2}{m}\right)^{1.43}, \qquad (5)$$

with units of years, solar masses and solar radii. We have applied this formula to the same models that we evolved without mass loss. For $M_i = 0.8$ and 1.0, we find that ΔW passes through zero on the FGB, as before, but that on the AGB the entire envelope is lost by stellar wind before reaching a point where $\Delta W = 0$. For $M_i \gtrsim 2\,M_\odot$, however, the effect of the JS stellar wind on the values of both M_s (the surface mass when $\Delta W = 0$) and M_f was insignificant.

Table 1 gives our M_i–M_f relation in the three cases (i) Pop I, no stellar wind, (ii) Pop I, stellar wind from JS, and (iii) Pop II, no stellar wind. In Table 2, we illustrate the effect of varying a number of assumptions: the JS mass-loss rate multiplied by 3; a Reimers (1975) wind with Reimers's parameter $\eta = 1/3$; Pop I with a higher H abundance ($X = 0.75$); Pop II with a lower H abundance ($X = 0.7$); convection with $\alpha = 2.5$ and 3. The last variation seems the most significant: M_f is increased by ~ 12 per cent at $M_i = 3\,M_\odot$.

An alternative, and in many respects more powerful, test of our hypothesis is to compare the distribution of masses of planetary nebula nuclei (PNN) that it predicts with the observed one. For this purpose, we have convolved our Pop I M_i–M_f relation with a distribution of initial masses (based on Scalo 1986) and an age of 20 Gyr, to find the expected distribution of PNN masses shown in Fig. 3(a) (using detailed Monte Carlo simulations). If we accept that the lowest mass stars really do lose their envelopes on the FGB, then we get a bimodal distribution, with the smaller peak at $0.46 \pm 0.01\,M_\odot$ and the larger peak (in terms of total number) at $0.60 \pm 0.02\,M_\odot$. The second peak has a long non-Gaussian tail towards high mass. This compares favourably with several observational estimates, for example those of Zhang & Kwok (1993), Kaler & Jacoby (1989) and Jacoby

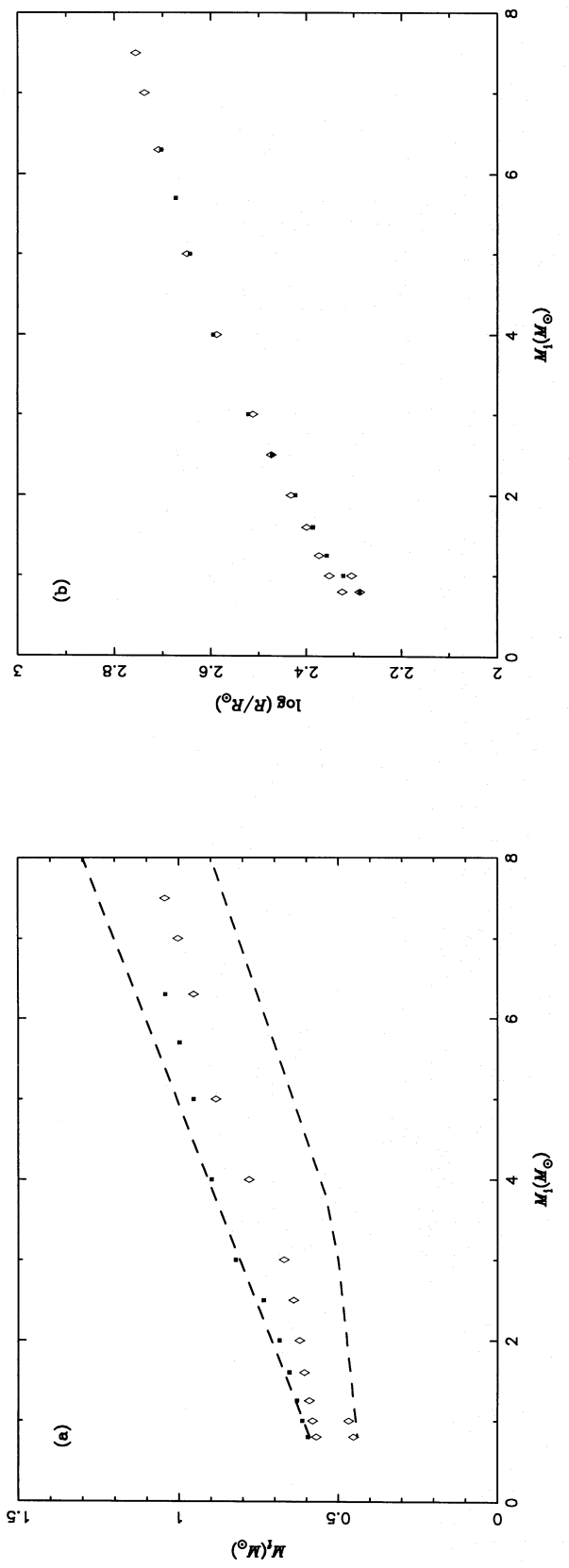

Figure 2. (a) Initial–final mass relations, (b) initial mass–final radius relations, (c) initial mass–final luminosity relations, and (d) the final position of FGB/AGB stars in the theoretical HRD (where $\Delta W = 0$). The diamonds and filled squares represent Pop I and Pop II stars, respectively. The observational initial–final mass relation by Weidemann & Koester (1983) lies between the two dashed lines in (a).

Table 1. Core masses, M_c, and surface masses, M_s, in solar units, when the envelope energy, ΔW, is zero. Pop I models are calculated with $X=0.70$, $Y=0.28$, $Z=0.02$ and $\alpha=2.0$, and Pop II models with $X=0.75$, $Y=0.25$, $Z=0.001$ and $\alpha=2.0$. All calculations use OPAL opacities at high temperatures and include molecular opacities at low temperatures. In cases where the envelope energy becomes positive on the first giant branch (FGB) and on the asymptotic giant branch (AGB), M_c (and M_s) is given at both evolutionary stages. Asterisks (*) indicate cases where the star loses all of its envelope in a stellar wind before it reaches $\Delta W=0$.

$M_i(M_\odot)$	0.80	1.00	1.25	1.60	2.00	2.50	3.00	4.00	5.00	5.70	6.30	7.00	7.50
Population I – no stellar wind													
M_c (FGB)		0.4520	0.4673										
M_c (AGB)	0.5695	0.5813	0.5918	0.6067	0.6218	0.6408	0.6707	0.7810	0.8848		0.9541	1.0027	1.0441
Population I – Judge and Stencel's stellar wind													
M_c (FGB)		0.4350	0.4551										
M_s (FGB)		0.6087	0.8557										
M_c (AGB)	0.46*	0.58*	0.5841	0.6043	0.6206	0.6385	0.6668	0.7814	0.8833		0.9549	1.0026	
M_s (AGB)	0.46*	0.58*	1.0812	1.5018	1.9374	2.4528	2.9629	3.9872	4.9906		6.2907	6.9947	
Population II, no stellar wind													
M_c (AGB)	0.5957	0.6128	0.6303	0.6544	0.6853	0.7352	0.8226	0.8982	0.9551	0.9984	1.0421		

Table 2. Core masses, M_c, and surface masses, M_s, in solar units, when the envelope energy, ΔW, is zero for various different assumptions about the physical input parameters, as indicated; other parameters are the same as in Table 1.

$M_i(M_\odot)$	1.00	1.60	3.00	7.00	$M_i(M_\odot)$	0.80	1.00	1.60	2.00	3.00	5.00	7.00
Population I, no stellar wind					Population I, with $X=0.75$, $Y=0.23$							
M_c (FGB)	0.4673				M_c (FGB)		0.4737					
M_c (AGB)	0.5813	0.6067	0.6707	1.0027	M_c (AGB)		0.5738			0.6725		0.9688
Population I, with JS's stellar wind					Population II, with $X=0.70$, $Y=0.299$							
M_c (FGB)	0.4551				M_c (FGB)							
M_s (FGB)	0.8557				M_c (AGB)	0.6058	0.6232	0.6789	0.6946	0.8708	0.9899	
M_c (AGB)	0.58*	0.6043	0.6668	1.0026								
M_s (AGB)	0.58*	1.5018	2.9629	6.9947								
Population I, with 3 times JS's stellar wind					Population I, with convection parameter $\alpha=2.5$							
M_c (AGB)		0.5950			M_c (FGB)							
M_s (AGB)		1.2773			M_c (AGB)		0.5971					
Population I, with Reimer's stellar wind ($\eta=\frac{1}{3}$)					Population I, with convection parameter $\alpha=3.0$							
M_c (FGB)	0.4553				M_c (FGB)							
M_s (FGB)	0.8471				M_c (AGB)		0.6136			0.7507		1.0068
M_c (AGB)	0.5702		0.6674	1.0018								
M_s (AGB)	0.6801		2.9160	6.9415								

(1989), shown for comparison in Figs 3(b)–3(d). Our M_i–M_f relation also compares well with the two independent theoretical determinations by Vassiliadis & Wood (1993) and Wagenhuber & Weiss (1993) (see Table 3).

4 DISCUSSION AND IMPLICATIONS

4.1 The PN ejection mechanism

The good agreement between our calculations and observations, in particular for the distribution of PNN masses (Fig. 3b), strongly suggests that the ultimate cause for the envelope ejection in evolved giants is to be found in the positive binding energy of the envelope. This model does not, however, directly specify the actual ejection mechanism, for example whether it is dynamical ejection or rapid mass loss in a pulsationally driven superwind. Earlier investigation of this problem (see the references in Wagenhuber & Weiss 1993, and Vassiliadis & Wood 1993) have remained largely inconclusive, mainly because of technical limitations. Recently, Wagenhuber & Weiss (1993) argued that a single thermal pulse can initiate a runaway expansion driven by the recombination of hydrogen and helium and leading to the fast ejection of the envelope. Alternatively, the point at which the envelope binding energy becomes positive may determine

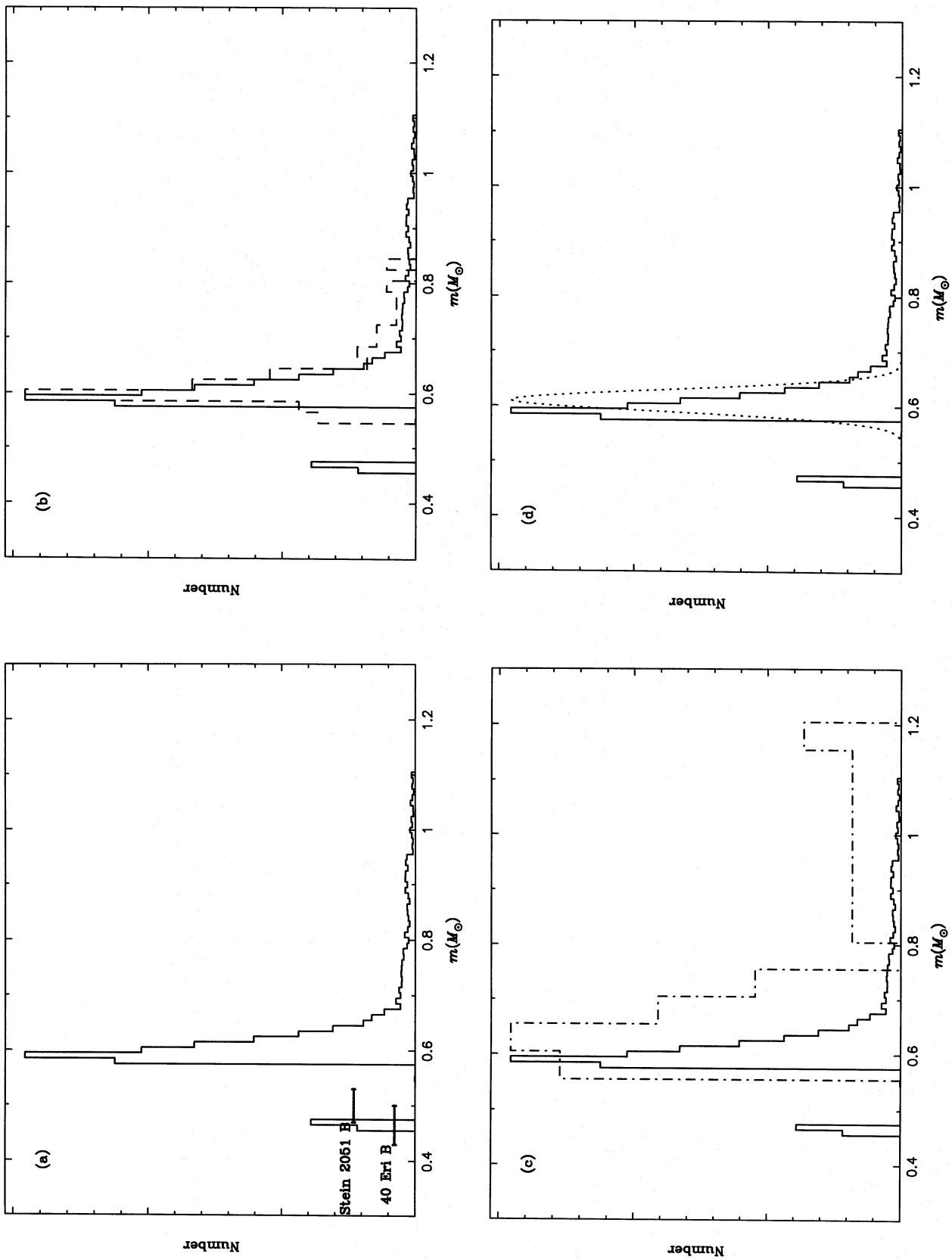

Figure 3. (a) The expected mass distribution, $dN(m)/dm$, of planetary nebula nuclei (PNN) (solid line), which results from the convolution of our Pop I initial–final mass relation with an IMF based on Scalo (1986) for an age of 20 Gyr. For comparison, (b) shows the observational PNN mass distribution from Zhang & Kwok (1993) (dashed line), (c) shows the distribution from Kaler & Jacoby (1989) (dot–dashed line), and (d) shows the distribution inferred observationally by Jacoby (1989) (dotted line). The positions of Stein 2051 B and 40 Eri B are also shown in (a).

Table 3. The initial–final mass relations by Vassiliadis & Wood (1993) and Wagenhuber & Weiss (1993). The results of Vassiliadis & Wood (1993) are based on an observational calibration of superwind mass-loss rates. Wagenhuber & Weiss (1993) consider the dynamical ejection of AGB envelopes during individual thermal pulses (for a variety of input assumptions). The asterisks (***) indicate initial masses for which no dynamical instabilities were encountered by Wagenhuber & Weiss (1993).

$M_i(M_\odot)$	0.8	1.0	1.2	1.5	2.0	2.5	3.5	4.0	5.0
Vassiliadis and Wood (1993)									
$M_f(M_\odot)$		0.568		0.600	0.633	0.666	0.751		0.891
Wagenhuber and Weiss (1993)									
$M_f(M_\odot)$	***	0.5704	0.5835	0.6025		0.7590		0.8690	***
$M_f(M_\odot)$		0.5702	0.5879	0.6075		0.6798			
$M_f(M_\odot)$		0.5714	0.5929			0.6935			

the onset of a pulsationally driven (Mira) superwind (also see Vassiliadis & Wood 1993). In the latter case, the mass of the degenerate core can still increase between the onset of the instability and the complete ejection of the envelope. We can estimate the increase in the core mass, ΔM_c, during a superwind phase from $\Delta M_c \simeq \dot{M}_c(M_{env}/\dot{M}_{SW})$. Here, the core growth rate $\dot{M}_c$ can be approximately related to the luminosity L by $\dot{M}_c \simeq L/0.008c^2$, M_{env} is the envelope mass, and $\dot{M}_{SW}$ the superwind mass-loss rate. Adopting a typical superwind mass-loss rate $\dot{M}_{SW} \sim 5\times10^{-5}\,M_\odot\ yr^{-1}$ (Vassiliadis & Wood 1993) and using our stellar models, we find an increase of the core mass of $\sim 3\times10^{-4}M_\odot$ for a 1.25-$M_\odot$ model, and of $\sim 0.04\,M_\odot$ for a 7-$M_\odot$ model. Thus the increase of the core mass during a superwind phase is completely negligible at low masses and relatively modest at high masses. More importantly, these estimates also suggest that the location of the peak in the predicted white dwarf distribution is not very sensitive to the actual ejection mechanism.

4.2 White dwarf masses and supernovae

The results of our calculations have important implications for a variety of astrophysical problems.

First, they suggest that Pop I stars with masses less than $\sim 1\,M_\odot$ may eject their envelopes already on the first red giant branch (Table 1), probably at the helium flash which could provide the ejection mechanism. This behaviour may in fact be required to explain the low masses of the white dwarfs in Stein 2051 B and 40 Eri B, which are consistent with He white dwarfs but seem to be too low for the cores of AGB stars. Both of these white dwarfs are in sufficiently wide orbits ($\sim$350 and 250 yr respectively: van de Kamp 1971) that there should have been no binary interaction in the past; the length of these orbits, however, each of which has been observed for only a fraction of one orbit, also makes the masses quite uncertain. In contrast to Pop I, our Pop II stars with masses as low as $0.6\,M_\odot$ did not reach the point where $\Delta W = 0$ on the FGB. Nevertheless, the envelopes of FGB stars may already be sufficiently loosely bound at the time of the helium flash to cause significant mass loss as a result of the flash. We note that it is difficult to test observationally whether low-mass, metal-rich stars evolve to the AGB, since there are few sufficiently old, metal-rich clusters in the Galaxy or the Magellanic Clouds – with the possible exception of the Galactic open clusters M67 and NGC 188 and some metal-rich globular clusters near the Galactic Centre (see e.g. Ortolani, Barbuy & Bica 1990); but the red giant branches in these, however, are too sparsely populated to allow the identification of an AGB (e.g. Tinsley & Gunn 1976; McClure & Twarog 1977). On the other hand, Dorman, Rood & O'Connell (1993) have recently suggested that the strong far-ultraviolet excess observed in metal-rich elliptical galaxies requires the presence of a population of extreme horizontal branch stars which have lost almost all of their envelopes on the FGB and never become AGB stars. This is consistent with our scenario, provided that most of the envelope mass is lost at the helium flash. Thus it remains an intriguing theoretical possibility, to be challenged observationally, that stars like the Sun may never become AGB stars.

The second implication of our results is that the maximum mass of a degenerate CO core formed in our models is $\sim 1.1\,M_\odot$ for a star with an initial mass somewhat less than $8\,M_\odot$ (its maximum luminosity during the AGB phase is $\sim 3\times10^4\,L_\odot$). Our 8-$M_\odot$ model ignites carbon off-centre in a mildly degenerate core. This is expected to lead to quiescent carbon burning (Iben 1974), and ultimately to a core-collapse supernova leaving a neutron star remnant (Hashimoto, Iwamoto & Nomoto 1993). Thus our calculations suggest that the degenerate CO core in an AGB star can never grow to reach the Chandrasekhar mass ($M_{Ch} \simeq 1.4\,M_\odot$), which would result in a thermonuclear explosion and the complete disruption of the star (a Type $1\frac{1}{2}$ supernova in the nomenclature of Iben & Renzini 1983). This is important for global chemical models of the Universe, since supernovae of this type, if they existed, would probably be the dominant producers of iron. In addition, there should be few CO white dwarfs with masses above $\sim 1.1\,M_\odot$, unless they accreted a significant amount of mass from a companion star. This has consequences for models in which neutron stars are formed by accretion-induced collapse and in which massive CO white dwarfs are potential progenitors (see e.g. Nomoto & Kondo 1991).

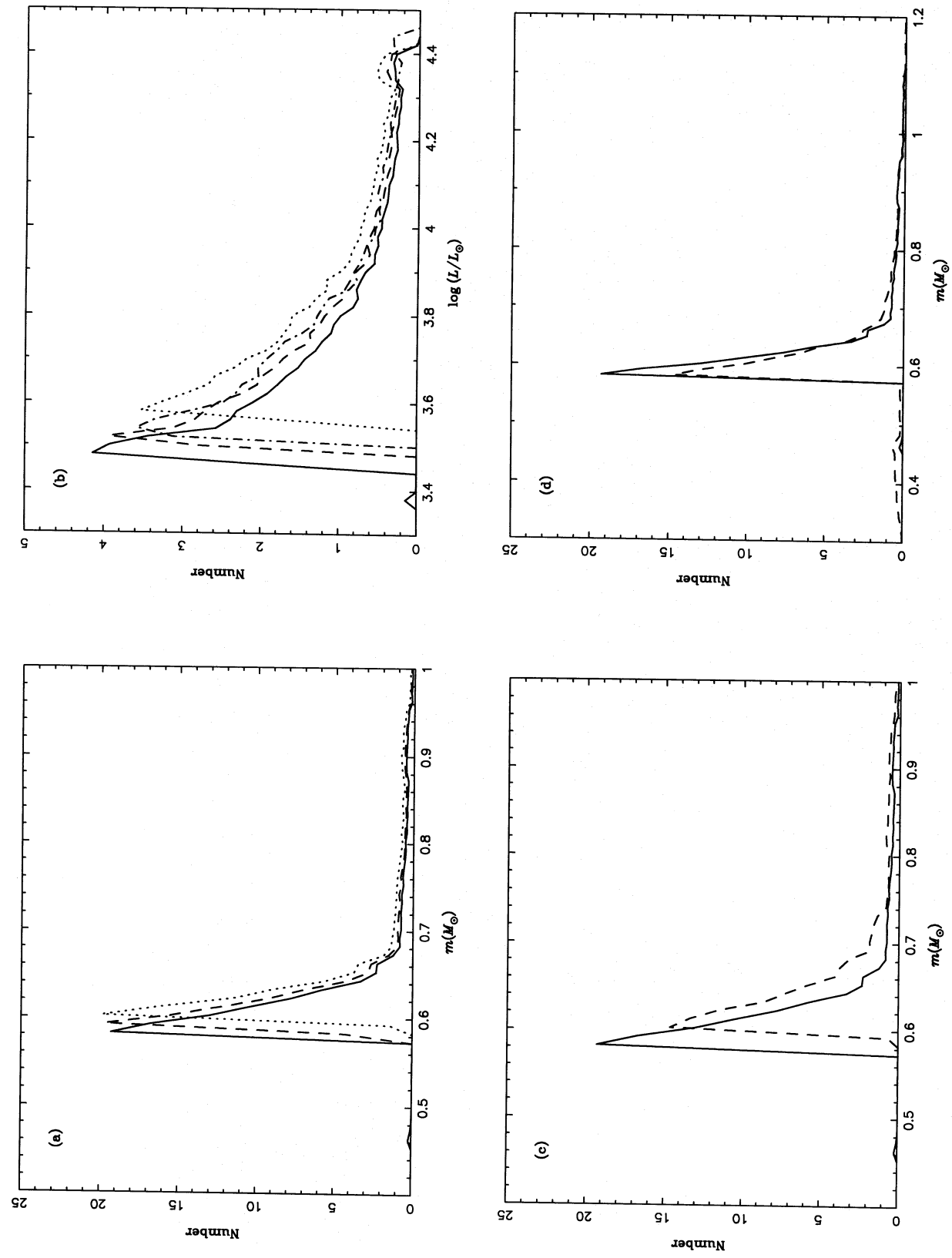

Figure 4. (a) The WD mass distributions, d$N(m)$/dm, for Pop I systems with ages of 15 Gyr (solid line), 10 Gyr (dashed line) and 5 Gyr (dotted line). (b) The luminosity distributions, d$N(L)$/d log L, for Pop I systems at the time of envelope ejection with ages of 15 Gyr (solid line), 10 Gyr (dashed line) and 5 Gyr (dotted line), and for Pop II systems with an age of 15 Gyr (dot–dashed line). (c) The WD mass distributions for Pop I systems (solid line) and Pop II systems (dashed line) with an age of 15 Gyr. (d) The WD mass distributions for Pop I systems with an age of 15 Gyr without binary interaction (solid line) and with binary interaction (dashed line).

4.3 Planetary nebulae as distance indicators

Perhaps the most important implication of our results is that they, possibly for the first time, provide strong *theoretical* support for using planetary nebulae (PNe) as reliable distance indicators (see Jacoby 1989). As shown by Jacoby (1989), the luminosity function of PNe can be used as a standard distance candle provided that the mass distribution for the central white dwarfs in PNe has a well-defined and narrow peak. Our results satisfy both of these requirements, and, in fact, the peak of our predicted white dwarf mass distribution is in excellent agreement with the distribution inferred observationally by Jacoby (1989) (see Fig. 3d).

In addition, our models allow us to investigate the dependence of the WD mass and luminosity distributions on the properties of the underlying stellar population, like age and metallicity, and the effects of binary interactions. In Fig. 4(a) we present the WD mass distributions for three Pop I systems with ages of 5, 10 and 15 Gyr. The peaks in the mass distribution are at 0.61 ± 0.02, 0.60 ± 0.02 and 0.59 ± 0.02 $M_\odot$, respectively. Note that the shapes of the peaks are highly non-Gaussian; the quoted range is defined to include half of all white dwarfs. The corresponding peaks in the luminosity distribution (in $\log L/L_\odot$) at the time of envelope ejection are at 3.66 ± 0.1, 3.59 ± 0.1 and 3.55 ± 0.1, respectively (Fig. 4b). Similarly, Fig. 4(c) compares the WD mass distribution for a Pop I system with that of a Pop II system (as defined in Table 1) with the same age of 15 Gyr. As expected from Table 1, the peak in the mass distribution for the Pop II system is shifted from 0.59 ± 0.02 $M_\odot$ to 0.62 ± 0.02 $M_\odot$. The corresponding peaks in the luminosity distributions are at 3.55 ± 0.1 and 3.61 ± 0.1, respectively (Fig. 4b). Finally, Fig. 4(d) illustrates the effects of including the consequences of binary interactions [based on a detailed binary population model described by Han, Podsiadlowski & Eggleton (in preparation)]. In this case, the main peak at 0.60 ± 0.025 $M_\odot$ is slightly broadened. In addition, there is a second very broad peak of He white dwarfs around 0.45 $M_\odot$, and the number of massive CO white dwarfs is also increased. Indeed, the most massive CO white dwarf formed as a result of mass transfer has a mass of ~ 1.2 $M_\odot$ instead of ~ 1.1 $M_\odot$, originating from a massive progenitor that filled its Roche lobe just before the second dredge-up.

In summary, these comparisons suggest a sharp peak in the luminosity distribution of AGB stars at the time of envelope ejection around 3800 $L_\odot$, which varies by less than ~ 20 per cent with the age and metallicity of the underlying population. To relate this to an uncertainty in distance determinations based on PN luminosity functions, one also has to take into account the various observational selection effects in the determination of PN luminosity functions; these will generally have a tendency to reduce the uncertainty. Irrespective of selection effects, our results suggest an intrinsic uncertainty in PN distance determinations of less than ~ 10 per cent.

REFERENCES

Andersen J., 1991, A&AR, 3, 91
Bessell M. S., Brett J. M., Scholz M., Wood P. R., 1989, A&AS, 77, 1
Biermann L., 1938, Z. Astrophys., 16, 29
Biermann L., Cowling T. G., 1939, Z. Astrophys., 19, 1
Christensen-Dalsgaard J., Gough D. O., Thompson M. J., 1991, ApJ, 378, 413
Dorman B., Rood R. T., O'Connell R. W., 1993, ApJ, 419, 596
Eggen O. J., 1985, AJ, 90, 333
Eggleton P. P., 1971, MNRAS, 151, 351
Eggleton P. P., 1972, MNRAS, 156, 361
Eggleton P. P., 1973, MNRAS, 163, 279
Eggleton P. P., 1983, MNRAS, 204, 449
Eggleton P. P., Faulkner J., Flannery B. P., 1973, A&A, 23, 325
Fowler W. A., Caughlan G. R., Zimmerman B. A., 1976, ARA&A, 13, 69
Hashimoto M., Iwamoto K., Nomoto K., 1993, ApJ, 414, L105
Hubbard W. B., Lampe M., 1969, ApJS, 18, 297
Iben I., Jr, 1974, ARA&A, 12, 215
Iben I., Jr, Renzini A., 1983, ARA&A, 21, 271
Jacoby G. H., 1989, ApJ, 339, 39
Judge P. G., Stencel R. E., 1991, ApJ, 371, 357 (JS)
Kaler J. B., Jacoby G. H., 1989, ApJ, 362, 491
Koester D., 1972, A&A, 16, 459
Lucy L. B., 1967, AJ, 72, 813
McClure R. D., Twarog B. A., 1977, ApJ, 214, 111
Maeder A., Mermilliod J. C., 1981, A&A, 93, 136
Nomoto K., Kondo Y., 1991, ApJ, 367, L19
Ortolani S., Barbuy B., Bica E., 1990, A&A, 236, 362
Paczyński B., 1976, in Eggleton P. P., Mitton, Whelan, eds, Proc. IAU Symp. 73, Structure and Evolution of Close Binary Systems, p. 75
Paczyński B., Ziółkowski J., 1968, Acta Astron., 18, 255 (PZ)
Reimers D., 1975, Mem. R. Soc. Liège, 6ième Serie, 8, 369
Rogers R. J., Iglesias C. A., 1992, ApJS, 79, 507 (OPAL)
Roxburgh I. W., 1967, Nat, 215, 838
Schwarzschild M., Härm R., 1965, ApJ, 142, 855
Scalo J. M., 1986, Fundam. Cosmic Phys., 11, 1
Shklovskii I. S., 1956, AZh, 33, 315
Tinsley B. M., Gunn J. E., 1976, ApJ, 206, 525
van de Kamp P., 1971, ARA&A, 9, 103
Vassiliadis E., Wood P. R., 1993, ApJ, 413, 641
Wagenhuber J., Weiss A., 1993, A&A, preprint
Weidemann V., Koester D., 1983, A&A, 121, 77 (WK)
Weiss A., Keady J. J., Magee N. H., Jr, 1990, At. Data Nucl. Data Tables, 45, 209 (WKM)
Zhang C. Y., Kwok S., 1993, ApJS, 88, 137